

Combining tissue clearing and Fluoro-Jade C labeling for neurotoxicity assessments

Qiang Gu , Sumit Sarkar, Bryan Raymick and Jyotshna Kanungo

Division of Neurotoxicology, National Center for Toxicological Research, U.S. Food and Drug Administration, Jefferson, AR 72079, USA
Corresponding author: Qiang Gu. Email: qiang.gu@fda.hhs.gov

Impact Statement

Tissue-clearing techniques use chemical means to remove light-scattering and light-absorbing molecules from the tissue and make the tissue transparent for subsequent imaging analyses. While tissue clearing has been successfully applied in some studies, little is known about the utilization of this technique for neurotoxicity assessments. In this study, several tissue-clearing methods were assessed in combination with Fluoro-Jade C (FJ-C), a standard marker of neurodegeneration. The results suggest that some but not all tissue-clearing media are compatible with the FJ-C fluorophore and that FJ-C labeling can be combined with tissue clearing for neurotoxicity assessments. This approach could be further expanded by combining multicolor labeling of molecular targets involved in various neurological pathologies. This study is the first to show the combined use of tissue clearing and FJ-C for neurotoxicity assessment. It is anticipated that this combined approach would be an added tool for the detection and evaluation of neurotoxicity and neurodegeneration.

Abstract

Tissue clearing refers to laboratory methods that make tissue transparent by chemical means. This approach allows the labeling, visualization, and analysis of specific targets without cutting the tissue into sections, thereby maintaining three-dimensional architecture. More than two dozen tissue-clearing methods have been developed by different research teams to date. While tissue clearing has been successfully applied in several studies concerning basic science or diseases, little is known about the utilization of tissue clearing for neurotoxicity evaluation. In this study, several tissue-clearing methods were combined with Fluoro-Jade C (FJ-C), a standard marker of neurodegeneration. The results suggest that some but not all tissue-clearing media are compatible with the FJ-C fluorophore. By utilizing a neurotoxicity animal model, the results further suggest that FJ-C labeling can be combined with tissue clearing for neurotoxicity assessments. This approach has the potential to be expanded further by combining multicolor labeling of molecular targets involved in the development and/or mechanisms of neurotoxicity and neurodegeneration.

Keywords: Tissue clearing, Fluoro-Jade C, neurotoxicity, neurodegeneration, fluorescence labeling, kainic acid

Experimental Biology and Medicine 2023; 248: 605–611. DOI: 10.1177/15353702231165009

Introduction

Tissue clearing removes light-scattering and light-absorbing components from body tissues, homogenizing the refractive index of the tissue,^{1–3} allows the visualization of molecular targets in intact organs, and can reduce background noise in tissue samples for fluorescence imaging. The visualization of molecular targets in tissue-cleared organs can be achieved through different fluorescence-based approaches such as germline manipulation (transgenic expression), genetic labeling (viral vector insertion), immune-conjugated fluorophores, chemical probes or tracers, and nucleic acid site-specific detection.⁴ Tissue clearing has been increasingly utilized in broad scientific disciplines, most notably neuroscience, developmental biology, cancer research, stem cell research, and even in organoids and three-dimensional (3D)

cell cultures.^{5–13} Most tissue-clearing studies in neuroscience have focused on the validation of specific tissue-clearing methods, addressing basic neuroscience issues such as location and developmental expression of specific proteins in the nervous system, or identifying molecular changes associated with neurological diseases or neurodegenerative disorders.⁶ However, little is known about the application of tissue clearing for neurotoxicity assessments. Therefore, this study focused on evaluating the feasibility and usefulness of tissue-clearing techniques in neurotoxicity assessments. Histopathological assessments of neurotoxicity typically involve histochemical or immunocytochemical methods, which utilize chromophores or fluorophores to label target molecules in the brain as signs or biomarkers of toxicity. Since tissues contain light-scattering (e.g. lipids) and light-absorbing (e.g. pigments) components, a light beam can only

penetrate a limited distance into the tissue. Therefore, the brain must be cut into thin tissue sections for conventional histopathological examinations. Tissue-clearing approaches, by contrast, remove light-scattering and light-absorbing components from tissue and make tissue transparent, so labeled targets deep inside the brain can be observed without cutting the brain into sections. For instance, using fluorescent markers to label endothelial cells of the blood-brain barrier and combined with light-sheet microscopy, tissue clearing could allow imaging and quantification of the entire vascular network in the whole brain without tissue sectioning.⁵ More than two dozen tissue-clearing methods have been developed to date and based on the chemicals employed, they can be categorized into three main groups: organic solvent-based, aqueous hyperhydrating-based, and hydrogel-embedded.^{6,9,14,15} To aim a broad applicability, this study examined all three types of tissue-clearing methods.

Fluoro-Jade C (FJ-C) is a fluorescent tracer derived from fluorescein and has been widely used for histochemical labeling of degenerating neurons.¹⁶ Compared to its two predecessors, Fluoro-Jade¹⁷ and Fluoro-Jade B,¹⁸ FJ-C results in tissue staining with higher resolution, higher contrast, and lower background noise.¹⁹ FJ-C labeling has been applied in a variety of studies such as traumatic brain injury, developmental apoptosis, ischemia, and animal models of neurodegenerative diseases and assessing neurotoxicity.^{16,19–28} The FJ-C stain is among a few techniques commonly used for neurotoxicity assessment. The current histopathological evaluation of neurotoxicity is based on the observation of only a few tissue sections because it is impractical to cut the entire brain into sections of appropriate thickness and examine all of them.²⁹ However, if a specific brain region is injured by drug treatment or disease state but is not included in those few tissue sections selected for examination, then false-negative outcomes can occur. If FJ-C can be combined with tissue clearing techniques for the detection of degenerating neurons, it would allow visualization of FJ-C-labeled cells in tissue-cleared brain samples without sectioning the tissue, possibly allowing for a more efficient and thorough assessment of neurotoxicity in both preclinical animal models and postmortem human brain samples. Since FJ-C labeling has never been evaluated in conjunction with any tissue-clearing application previously, and since different tissue-clearing methods possess different characteristics in terms of the complexity, efficiency, speed, tissue volume change, and so on, this study was designed to address the following questions: (1) is the FJ-C fluorophore resistant to tissue-clearing reagents or incubation media? (2) could tissue-clearing procedures destroy the FJ-C fluorophore and/or FJ-C binding targets in the tissue? (3) can FJ-C labeling be successfully performed in tissue-cleared brain samples? and (4) can FJ-C be combined with tissue-clearing techniques for neurotoxicity assessments? To test this concept, animals that received intraperitoneal injections of kainic acid (KA) as a model of neurotoxicity were subjected to FJ-C labeling,¹⁹ tissue clearing, and fluorescence imaging, using representative methods from each of the three major chemical categories, that is, organic solvent-based, aqueous hyperhydrating-based, and hydrogel-embedded tissue clearing.

Materials and methods

Animal treatment and tissue preparation

All animal procedures were approved by the Institutional Animal Care and Use Committee. Animals were purchased from commercial vendors: adult male Sprague Dawley rats from Envigo RMS, LLC (Indianapolis, IN, USA) and six-week-old male C57BL/6J mice from The Jackson Laboratory (Bar Harbor, ME, USA). Animals were acclimated for at least one week before any experiment. To induce neurotoxicity in the brain, animals were treated with intraperitoneal (i.p.) injections of KA (10 mg/kg bodyweight of rats or 30 mg/kg bodyweight of mice). Animals receiving i.p. injections of saline (same volume as calculated for KA) were used as controls. Possible behavioral changes in the KA-treated animals included grooming, rearing, hind limb scratching, wet dog shakes, jaw movements, salivation, urination, defecation, head nodding, and seizures. Animals experiencing severe seizures, reflected by repeated falls, were injected with pentobarbital (17 mg/kg, i.p.) to stop seizures and prevent potential animal death. Twenty-four hours after KA- or saline-injection, animals were euthanized by i.p. injection of pentobarbital (100 mg/kg bodyweight), perfused with 0.1 M phosphate buffer saline (PBS) to remove blood cells from the vasculature, and followed by 4% paraformaldehyde (PFA) for 5 min. After perfusion, brain samples were collected and postfixed in PFA at 4°C until use.

To confirm that KA-treated animals developed the desired neurotoxicity, fixed brains were cut in the sagittal plane to make equal left and right hemispheres. One hemisphere was used for the conventional FJ-C labeling analysis to confirm positive FJ-C labeling in those KA-treated brain samples, while the other hemisphere was used for tissue clearing. Various thicknesses of tissue sections from 25 µm to 1 mm were obtained by means of a cryostat (Leica CM3050S, Nussloch, Germany) or a vibratome (Ted Pella DTK-3000W, Redding, CA, USA). All tissue samples were washed in PBS at room temperature to remove fixative before further processing.

Tissue clearing

The tissue-clearing methods were adopted from the established protocols. Therefore, the tissue-clearing procedures are only briefly described here with references to associated publications. All incubations were conducted at room temperature unless otherwise specified. The total time required to clear each tissue sample varied by tissue-clearing methods as well as size and thickness of the tissue samples.

BABB (Benzyl alcohol-benzyl benzoate). Tissue samples were dehydrated in a graded ethanol series (30%, 50%, 70%, 80%, 96%, and twice in 100%), and then rinsed in 100% hexane for 1 h.³⁰ Tissue samples were transferred into a clearing solution containing benzyl alcohol and benzyl benzoate (BABB) (ratio 1:2) until samples became transparent.

CUBIC (Clear, unobstructed brain/body imaging cocktails). Tissue samples were immersed in 1:1 water-diluted CUBIC-L (TCI America, Portland, OR, USA) at 37°C for

3h.³¹ The 50% CUBIC-L was then discarded, and 100% CUBIC-L was added. Tissue samples were gently shaken at 37°C overnight; the incubation reagent was replaced every two days until samples became transparent. Tissue samples were then immersed in CUBIC-R (TCI America) and gently shaken at room temperature overnight. The next day, the reagent was replaced with fresh reagent and further incubated for 24 h.

pClarity (Passive clarity). Tissue samples were incubated in a borate-SDS (sodium dodecyl sulfate) buffer containing 200 mM boric acid, 4% SDS, and 20 mM lithium hydroxide monohydrate (pH 8.5) at 37°C until tissue became transparent.³²

RTF (Rapid clearing method based on Triethanolamine and Formamide). Tissue samples were incubated in RTF-R1 (30% triethanolamine, 40% formamide, and 30% dH₂O) for 2–3 h, in RTF-R2 (60% triethanolamine, 25% formamide, and 15% dH₂O) for 2–3 h, and in RTF-R3 (70% triethanolamine, 15% formamide and 15% dH₂O) for at least one day.³³

SeeDB2 (See deep brain 2). Tissue samples were incubated in 2% saponin (diluted in PBS) for 12–16 h, in the first tissue-clearing solution of 2% saponin and 1/3 SeeDB2G solution (Wako Chemicals USA, Richmond, VA, USA) in dH₂O for 6–10 h, in the second tissue-clearing solution (2% saponin and 1/2 SeeDB2G solution in dH₂O) for 6–10 h, and finally in SeeDB2G solution containing 2% saponin for at least 12 h.³⁴

uDISCO (Ultimate 3D imaging of solvent-cleared organs). Tissue samples were dehydrated through serial incubations in 30%, 50%, 70%, 80%, 90%, 96%, and 100% *tert*-butanol at 35°C, followed by immersion in dichloromethane (DCM) for 60 min to remove the lipids. Subsequently, tissue samples were incubated in BABB-DCM (ratio = 1:0.75) until samples became transparent.³⁵

Visikol-HISTO. Tissue samples were incubated in 50% methanol in PBS for 2 h, 80% methanol in PBS for 2 h, 100% methanol for 2 h, Visikol-HISTO-1 (Visikol Inc., Hampton, NJ, USA) for 24 h, and then in Visikol-HISTO-2 (Visikol Inc.) for 24 h.³⁶

FJ-C labeling and imaging. For conventional FJ-C labeling, the original protocol¹⁹ was used. In brief, tissue sections were washed in PBS, mounted on gelatin-coated glass slides, and air-dried on a slide warmer (60°C). The glass slides were immersed in basic alcohol for 5 min, in 70% ethanol for 2 min, in dH₂O for 2 min, in 0.06% potassium permanganate for 10 min, in dH₂O for 2 min, in 0.0001% F-J C solution (0.01% FJ-C stock solution in 0.1% acetic acid at a dilution ratio of 1:100) for 10 min, and in dH₂O for 2 × 2 min. The glass slides were then air-dried on a slide warmer at 60°C for 5 min, and coverslipped with DPX.

For FJ-C labeling in combination with tissue clearing, FJ-C was mixed in the final tissue-clearing media (1:100 dilution of 0.01% FJ-C stock solution). The tissue samples were incubated in this solution for the same length of time as the

tissue-clearing procedure. Image acquisitions were made using a Nikon Eclipse-E400 microscope and fluorescein-isothiocyanate (FITC) filter.

Results

To examine if FJ-C signal remained intact after coming in contact with different tissue-clearing reagents, FJ-C-labeled brain sections of KA-treated animals underwent different tissue-clearing methods. Three organic solvent-based (BABB, uDISCO, and Visikol-HISTO), three aqueous hyperhydrating-based (CUBIC, RTF, and SeeDB2), and one hydrogel-embedded (pClarity) clearing methods were examined. The results indicated that the fluorescent signal of FJ-C remained intact after incubation with the organic solvent-based methods BABB (Figure 1(A)), uDISCO (Figure 1(B)), and Visikol-HISTO (Figure 1(C)). Among the aqueous hyperhydrating-based methods, fluorescent signal remained intact after incubation with SeeDB2 (Figure 1(D)) but disappeared after incubation with RTF (Figure 1(E)). The CUBIC method employs two incubation media sequentially, CUBIC-L for tissue clearing and CUBIC-R for homogenizing refractive index of the tissue. While FJ-C-labeled cells remained visible after the incubation with CUBIC-L (Figure 1(F)), they disappeared after incubation with CUBIC-R (Figure 1(G)). Fluorescent signal was also lost after incubation with the hydrogel-embedded method pClarity (Figure 1(H)). The incubation temperature of the conventional pClarity method was at 37°C. To rule out the possibility that the destruction of FJ-C signal during pClarity incubation was not due to higher temperature but rather chemicals in the incubation medium, previously FJ-C-labeled tissue sections were also incubated with pClarity medium at room temperature. Again, FJ-C signals were gone after incubation (Figure 1(I)), suggesting that the disappearance of signal was due to chemicals in the incubation medium.

Histochemical labeling by FJ-C is based on affinity binding between FJ-C molecules and FJ-C labeling sites expressed in the tissue. When the FJ-C signal disappears after incubation with tissue-clearing media like in RTF and pClarity, the chemical reagents in the incubation media might have destroyed the FJ-C fluorophore or the FJ-C labeling targets in the tissue. To investigate this issue further, tissue sections that had previous FJ-C labeling signals that disappeared after incubation with RTF and pClarity, respectively, were then washed to remove the tissue-clearing reagents and subsequently stained with FJ-C. The results showed FJ-C-labeled cells again (Figure 2(A) and (B)). These data suggest that FJ-C labeling sites in the tissue samples after RTF and pClarity incubations remained intact and the media of RTF and pClarity only destroyed the FJ-C fluorophores.

The conventional FJ-C labeling method consists of a series of incubation steps and requires the use of basic alcohol, acetic acid, and potassium permanganate as incubation reagents.¹⁹ Since potassium permanganate can give tissues a dark-brown color, the use of potassium permanganate is at odds with the principle of tissue clearing. Therefore, alterations to traditional FJ-C labeling were considered. Previous work has shown that FJ-C labeling could be achieved without the use of basic alcohol, acetic acid, and potassium

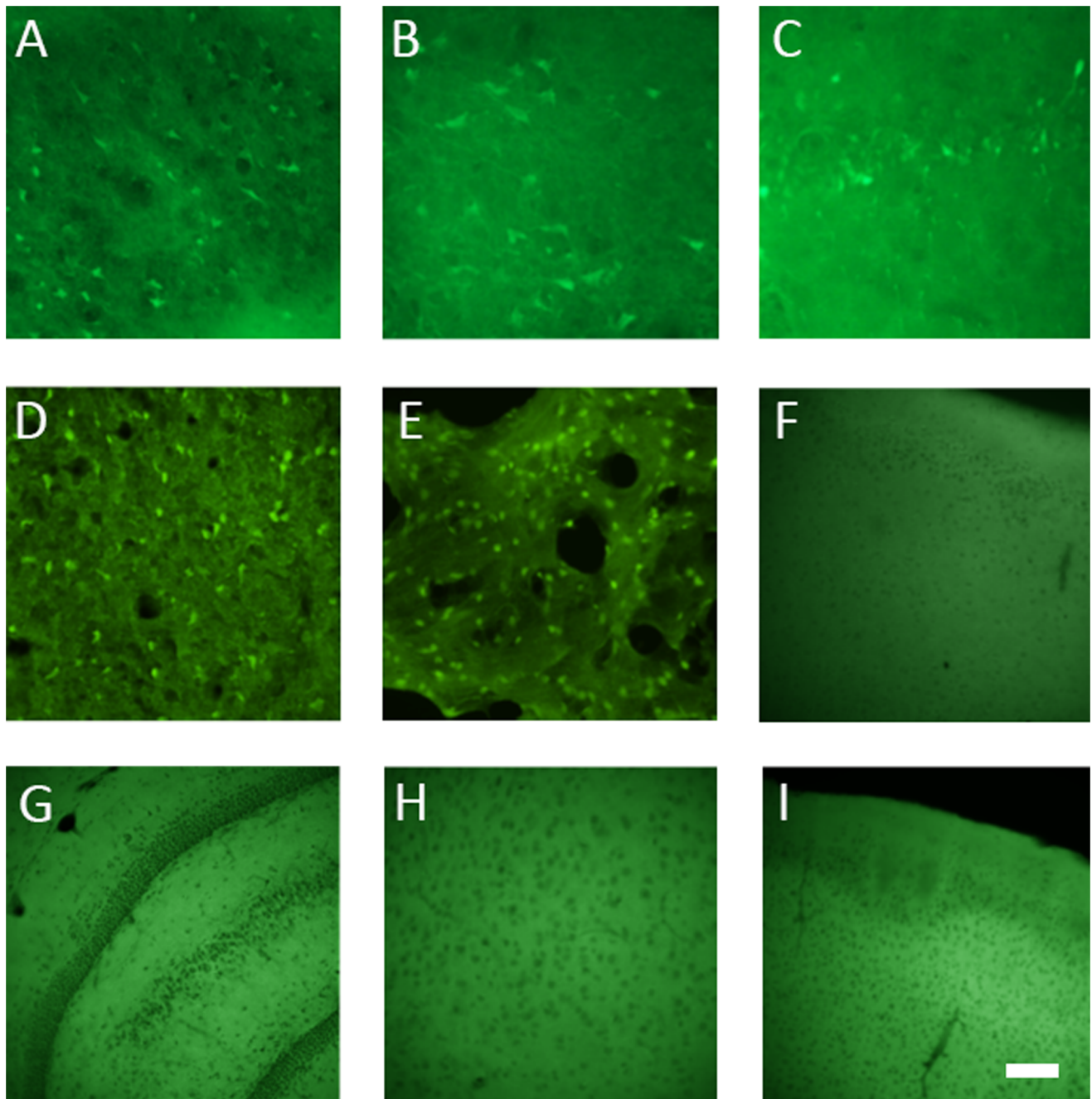


Figure 1. FJ-C labeling following incubation with organic solvent-based methods: BABB (A), uDISCO (B), and Visikol-HISTO (C); hyperhydrating-based methods: SeeDB2 (D), CUBIC-L (E), RTF (F), and CUBIC-R (G); and the hydrogel-embedded method pClarity with incubation temperature at 37°C (H) and at room temperature (I). Scale bar indicates 50 μ m for all panels.

permanganate.^{37,38} Therefore, a modified approach was tested by which FJ-C stock solution was directly diluted in the final tissue-clearing incubation media, so that tissue clearing and FJ-C labeling were run simultaneously. Based on the results of the compatibility tests above, the following tissue-clearing methods were examined: BABB, uDISCO, Visikol-HISTO, SeeDB2, and CUBIC-L. The results of the combined approaches revealed that brain tissue of KA-treated animals exhibited FJ-C-labeled neurons, while those of saline-treated control animals did not, after tissue clearing with BABB (Figure 3(A) and (B)), uDISCO (Figure 3(C)

and (D)), Visikol-HISTO (Figure 3(E) and (F)), CUBIC-L (Figure 3(G) and (H)), and SeeDB2 (Figure 3(I) and (J)).

Discussion

Tissue-clearing methods have been applied for fluorescence imaging of molecular targets in tissue samples such as endogenously expressed green fluorescence proteins (GFPs) or immunofluorescence-labeled proteins.⁴ However, the combination of tissue clearing and FJ-C labeling has not been reported previously. This study is the first to demonstrate

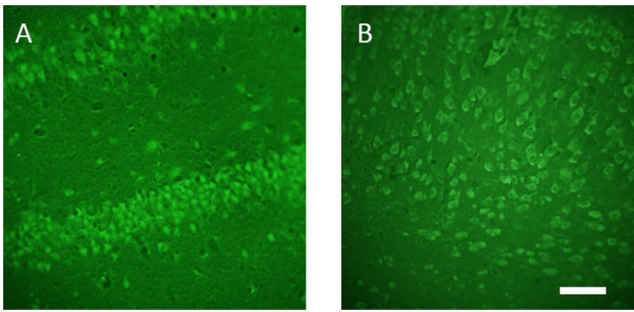


Figure 2. FJ-C labeling after RTF incubation, wash, and re-stain for FJ-C (A), and after incubation with pClarity, wash, and re-staining with FJ-C (B). Scale bar indicates 50 μ m for both panels. Because the RTF method can cause tissue shrinkage³³ and the pClarity method can cause tissue expansion,³² the labeled cells overall in (A) appear smaller than those in (B).

that FJ-C can be successfully combined with tissue clearing for the labeling of degenerating neurons. The fact that FJ-C could label neurons in KA-treated but not in saline-treated control tissue samples following tissue clearing suggests that FJ-C labeling remained specific for the detection of degenerating neurons in these combined approaches and tissue clearing did not produce FJ-C-labeled cells in the control tissue. Since FJ-C labeling has been widely applied in many different disease models of neurotoxicity or neurodegeneration, the combined usage of tissue clearing and FJ-C labeling should work in the other animal models as well. The limited scope of this study serves as a proof of concept, and further studies are needed to confirm the utility of the combined usage of tissue clearing and FJ-C labeling in other animal models, and even to expand to include postmortem human tissue samples as well as additional tissue-clearing methods.

Our data suggest that FJ-C is compatible with some but not all tissue-clearing reagents. Thus, when selecting a particular method for tissue clearing and FJ-C labeling, in addition to specific factors such as tissue-clearing speed and efficacy, the compatibility issue of FJ-C with tissue-clearing reagents should be considered or tested. Since the tissue-clearing incubation media may contain multiple chemical components, each single compound could be tested to determine which ones could destroy FJ-C fluorescence signal. The results could provide a practical guidance of FJ-C incompatible chemicals that should be avoided or substituted in tissue-clearing solutions. Alternatively, since there are several different tissue-clearing methods available to use, one could choose a tissue-clearing method from those that have been tested to be compatible with FJ-C, as presented in this study.

Taken together, our data show that all three tested organic solvent-based methods showed compatibility with FJ-C. Whether this could be generalized and applied to all organic solvent-based tissue-clearing methods that have been developed so far remains to be confirmed or contraindicated by additional studies. Concerning the aqueous hyperhydrating-based tissue-clearing methods, our results showed that FJ-C is compatible with SeeDB2 and CUBIC-L but not RTF and CUBIC-R. Since the purpose of CUBIC-R incubation is to homogenize the refractive index of the tissue, and is not directly involved in tissue clearing *per se*, CUBIC-R incubation may be omitted or substituted by another incubation

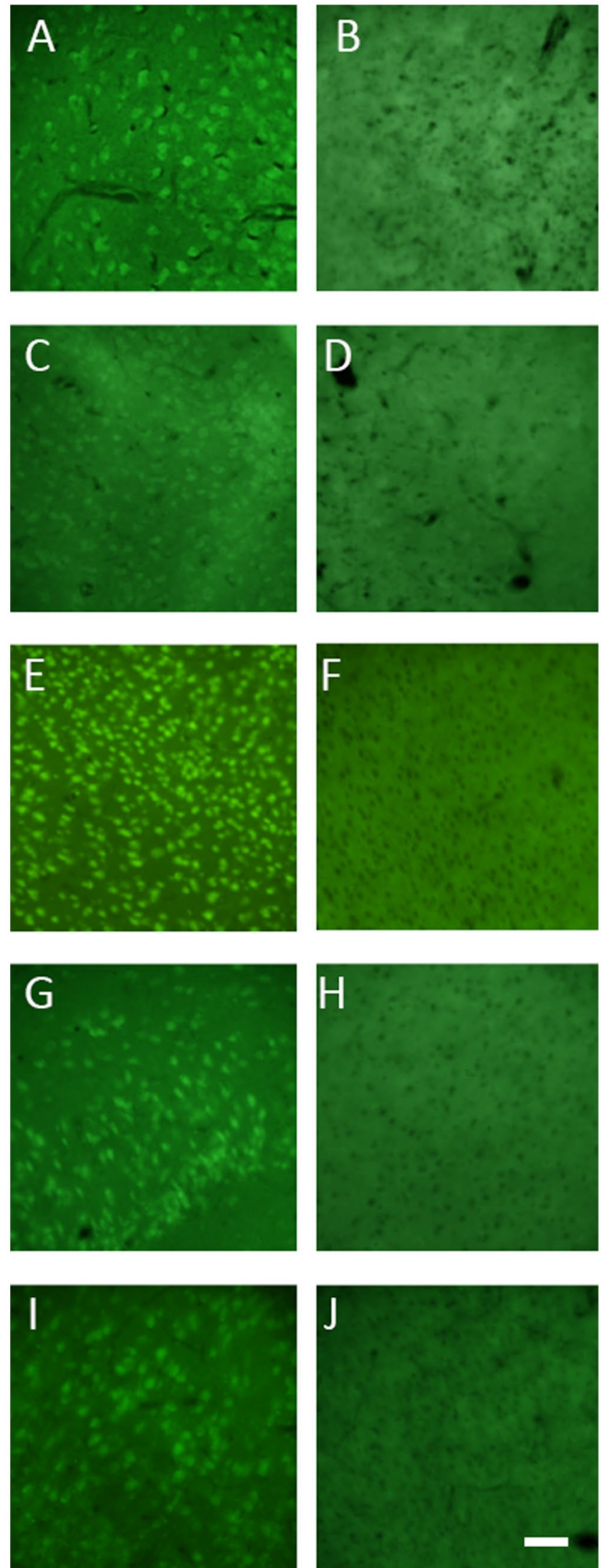


Figure 3. FJ-C labeling in tissue samples of KA- and saline-treated animals following incubation with FJ-C compatible tissue-clearing media: BABB (A and B), uDISCO (C and D), Visikol-HISTO (E and F), CUBIC-L (G and H), and SeeDB2 (I and J). Left and right panels represent KA- and saline-treatment, respectively. Scale bar indicates 50 μ m for all panels.

medium that could homogenize refractive index and is compatible with FJ-C. Although hydrogel-embedded tissue-clearing techniques have emerged with a few variations,³⁹ the core components remain the same, with differences in terms of (1) concentrations or ratios of chemical compounds, (2) whether using electrophoretic forces (active vs passive), (3) incubation times, and (4) incubation temperatures. Therefore, this study tested only one of them, pClarity, and the negative outcome of the pClarity test suggests that FJ-C may not be compatible with the incubation media of hydrogel-embedded tissue-clearing methods.

While the conventional FJ-C labeling requires the use of basic alcohol, acetic acid, and potassium permanganate, the modified approach in this study made FJ-C labeling much simpler by mixing FJ-C with the final tissue-clearing incubation media. This modification is based on previous observations that FJ-C labeling could be achieved without basic alcohol, acetic acid, and potassium permanganate.^{37,38} The successful combination of FJ-C with tissue clearing allows two processes, tissue clearing and FJ-C labeling, to run simultaneously, and thus, no extra time is needed for the FJ-C labeling procedure. The combined approach of tissue clearing and FJ-C labeling may be further expanded by adding additional molecular markers of interest for a multicolor labeling and imaging analysis.

In recent years, the light-sheet microscopy technique has been applied in studies to image tissue-cleared whole brains.^{4-6,12,40,41} The demonstration of the combined applications of tissue-clearing methods and FJ-C labeling in this study provided a foundation for future experiments that could make the visualization of FJ-C labeling in the entire brain after tissue clearing through a light-sheet imaging system possible. This combination would allow the acquisition of 3D images containing specific brain regions and molecular targets for a more thorough spatial and quantitative examination, and thus become a better tool for neurotoxicity assessment.

AUTHORS' CONTRIBUTIONS

QG, SS, and JK participated in the design and interpretation of the study. QG, SS, and BR conducted experiments. QG and JK analyzed the data. QG wrote the manuscript. All authors contributed to the manuscript revision.

ACKNOWLEDGEMENTS

This article reflects the views of the authors and does not necessarily reflect those of the US Food and Drug Administration.


DECLARATION OF CONFLICTING INTERESTS

The author(s) declared no potential conflicts of interest with respect to the research, authorship, and/or publication of this article.

FUNDING

The author(s) disclosed receipt of the following financial support for the research, authorship, and/or publication of this article: This work was supported by the U.S. Food and Drug Administration (FDA), National Center for Toxicological Research.

ORCID ID

Qiang Gu  <https://orcid.org/0000-0002-2606-0461>

REFERENCES

- Richardson DS, Lichtman JW. Clarifying tissue clearing. *Cell* 2015;**162**:246–57
- Azaripour A, Lagerweij T, Scharfbillig C, Jadczyk AE, Willershausen B, Van Noorden CJ. A survey of clearing techniques for 3D imaging of tissues with special reference to connective tissue. *Prog Histochem Cytochem* 2016;**51**:9–23
- Ariel P. A beginner's guide to tissue clearing. *Int J Biochem Cell Biol* 2017;**84**:35–9
- Newmaster KT, Kronman FA, Wu YT, Kim Y. Seeing the forest and its trees together: implementing 3D light microscopy pipelines for cell type mapping in the mouse brain. *Front Neuroanat* 2022;**15**:787601
- Kirst C, Skriabine S, Vieites-Prado A, Topilko T, Bertin P, Gerschenfeld G, Verny F, Topilko P, Michalski N, Tessier-Lavigne M, Renier N. Mapping the fine-scale organization and plasticity of the brain vasculature. *Cell* 2020;**180**:780–95
- Ueda HR, Ertürk A, Chung K, Gradinaru V, Chédotal A, Tomancak P, Keller PJ. Tissue clearing and its applications in neuroscience. *Nat Rev Neurosci* 2020;**21**:61–79
- Kim IK, Park JH, Kim B, Hwang KC, Song BW. Recent advances in stem cell therapy for neurodegenerative disease: three dimensional tracing and its emerging use. *World J Stem Cells* 2021;**13**:1215–30
- Liang X, Luo H. Optical tissue clearing: illuminating brain function and dysfunction. *Theranostics* 2021;**11**:3035–51
- Tian T, Yang Z, Li X. Tissue clearing technique: recent progress and biomedical applications. *J Anat* 2021;**238**:489–507
- Vieites-Prado A, Renier N. Tissue clearing and 3D imaging in developmental biology. *Development* 2021;**148**:dev199369
- Zhao J, Lai HM, Qi Y, He D, Sun H. Current status of tissue clearing and the path forward in neuroscience. *ACS Chem Neurosci* 2021;**12**:5–29
- Zhu J, Liu X, Deng Y, Li D, Yu T, Zhu D. Tissue optical clearing for 3D visualization of vascular networks: a review. *Vascul Pharmacol* 2021;**141**:106905
- Brenna C, Simioni C, Varano G, Conti I, Costanzi E, Melloni M, Neri LM. Optical tissue clearing associated with 3D imaging: application in preclinical and clinical studies. *Histochem Cell Biol* 2022;**157**:497–511
- Choi SW, Guan W, Chung K. Basic principles of hydrogel-based tissue transformation technologies and their applications. *Cell* 2021;**184**:4115–36
- Weiss KR, Voigt FF, Shepherd DP, Huisken J. Tutorial: practical considerations for tissue clearing and imaging. *Nat Protoc* 2021;**16**:2732–48
- Schmued LC. Development and application of novel histochemical tracers for localizing brain connectivity and pathology. *Brain Res* 2016;**1645**:31–5
- Schmued LC, Albertson C, Slikker W Jr. Fluoro-Jade: a novel fluorochrome for the sensitive and reliable histochemical localization of neuronal degeneration. *Brain Res* 1997;**751**:37–46
- Schmued LC, Hopkins KJ. Fluoro-Jade B: a high affinity fluorescent marker for the localization of neuronal degeneration. *Brain Res* 2000;**874**:123–30
- Schmued LC, Stowers CC, Scallet AC, Xu L. Fluoro-Jade C results in ultra-high resolution and contrast labeling of degenerating neurons. *Brain Res* 2005;**1035**:24–31
- He Z, Crook JE, Meschia JF, Brott TG, Dickson DW, McKinney M. Aging blunts ischemic-preconditioning-induced neuroprotection following transient global ischemia in rats. *Curr Neurovasc Res* 2005;**2**:365–74
- Bowyer JF, Ali S. High doses of methamphetamine that cause disruption of the blood-brain barrier in limbic regions produce extensive neuronal degeneration in mouse hippocampus. *Synapse* 2006;**60**:521–32
- Lee ST, Chu K, Park JE, Kang L, Ko SY, Jung KH, Kim M. Memantine reduces striatal cell death with decreasing calpain level in 3-nitropropionic model of Huntington's disease. *Brain Res* 2006;**1118**:199–207

23. Slikker W Jr, Zou X, Hotchkiss CE, Divine RL, Sadovova N, Twaddle NC, Doerge DR, Scallet AC, Patterson TA, Hanig JP, Paule MG, Wang C. Ketamine-induced neuronal cell death in the perinatal rhesus monkey. *Toxicol Sci* 2007;**98**:145–58
24. Chidlow G, Wood JP, Sarvestani G, Manavis J, Casson RJ. Evaluation of Fluoro-Jade C as a marker of degenerating neurons in the rat retina and optic nerve. *Exp Eye Res* 2009;**88**:426–37
25. Fritsch B, Qashu F, Figueiredo TH, Aroniadou-Anderjaska V, Rogawski MA, Braga MF. Pathological alterations in GABAergic interneurons and reduced tonic inhibition in the basolateral amygdala during epileptogenesis. *Neuroscience* 2009;**163**:415–29
26. Hoane MR, Kaufman N, Vitek MP, McKenna SE. COG1410 improves cognitive performance and reduces cortical neuronal loss in the traumatically injured brain. *J Neurotrauma* 2009;**26**:121–9
27. Sarkar S, Schmued L. Kainic acid and 3-nitropropionic acid induced expression of laminin in vascular elements of the rat brain. *Brain Res* 2010;**1352**:239–47
28. Lu E, Sarkar S, Raymick J, Paule MG, Gu Q. Decreased Mcl-1 protein level in the striatum of 1-methyl-4-phenyl-1,2,3,6-tetrahydropyridine (MPTP)-treated mice. *Brain Res* 2018;**1678**:432–9
29. Rao DB, Little PB, Malarkey DE, Herbert RA, Sills RC. Histopathological evaluation of the nervous system in national toxicology program rodent studies: a modified approach. *Toxicol Pathol* 2011;**39**:463–70
30. Dodt HU, Leischner U, Schierloh A, Jährling N, Mauch CP, Deininger K, Deussing JM, Eder M, Zieglgänsberger W, Becker K. Ultra-microscopy: three-dimensional visualization of neuronal networks in the whole mouse brain. *Nat Methods* 2007;**4**:331–6
31. Susaki EA, Tainaka K, Perrin D, Yukinaga H, Kuno A, Ueda HR. Advanced CUBIC protocols for whole-brain and whole-body clearing and imaging. *Nat Protoc* 2015;**10**:1709–27
32. Mortazavi F, Stankiewicz AJ, Zhdanova IV. Looking through brains with fast passive CLARITY: zebrafish, rodents, non-human primates and humans. *Bio Protoc* 2019;**9**:e3321
33. Yu T, Zhu J, Li Y, Ma Y, Wang J, Cheng X, Jin S, Sun Q, Li X, Gong H, Luo Q, Xu F, Zhao S, Zhu D. RTF: a rapid and versatile tissue optical clearing method. *Sci Rep* 2018;**8**:1964
34. Ke MT, Nakai Y, Fujimoto S, Takayama R, Yoshida S, Kitajima TS, Sato M, Imai T. Super-resolution mapping of neuronal circuitry with an index-optimized clearing agent. *Cell Rep* 2016;**14**:2718–32
35. Pan C, Cai R, Quacquarelli FP, Ghasemigharagoz A, Loubopoulos A, Matryba P, Plesnila N, Dichgans M, Hellal F, Ertürk A. Shrinkage-mediated imaging of entire organs and organisms using uDISCO. *Nat Methods* 2016;**13**:859–67
36. Merz G, Schwenk V, Shah RG, Necaie P, Salafia CM. Clarification and 3-D visualization of immunolabeled human placenta villi. *Placenta* 2017;**53**:36–9
37. Gu Q, Schmued LC, Sarkar S, Paule MG, Raymick B. One-step labeling of degenerative neurons in unfixed brain tissue samples using Fluoro-Jade C. *J Neurosci Methods* 2012;**208**:40–3
38. Gu Q, Lantz-McPeak S, Rosas-Hernandez H, Cuevas E, Ali SF, Paule MG, Sarkar S. In vitro detection of cytotoxicity using FluoroJade-C. *Toxicol in Vitro* 2014;**28**:469–72
39. Guo Z, Zheng Y, Zhang Y. CLARITY techniques based tissue clearing: types and differences. *Folia Morphol* 2022;**81**:1–12
40. Corsetti S, Gunn-Moore F, Dholakia K. Light sheet fluorescence microscopy for neuroscience. *J Neurosci Methods* 2019;**319**:16–27
41. Molbay M, Kolabas ZI, Todorov MI, Ohn TL, Ertürk A. A guidebook for DISCO tissue clearing. *Mol Syst Biol* 2021;**17**:e9807

(Received February 13, 2023, Accepted March 2, 2023)